





Experimental Investigation of Seawater for the Absorption of Carbon Dioxide from Ship Chimneys

İrem Koçyiğit Çapoğlu¹ , Duygu Uysal² , Özkan Murat Doğan³ , Bekir Zühtü Uysal⁴ 

^{1,2,3,4}Department of Chemical Engineering, Faculty of Engineering, Gazi University, Ankara, Türkiye

Abstract – Carbon dioxide (CO₂) is the most important greenhouse gas that causes global warming. It is crucial to remove CO₂ from the atmosphere to combat climate change. It is believed that seawater could be a potential source for capturing CO₂, especially from ship chimneys and potentially high-concentration CO₂ emissions in coastal regions. In this study, the CO₂ absorption performance of sodium chloride (NaCl) solution as seawater, was investigated. The first phase of experiments was performed in a stirred cell at 91 kPa and 20°C. The total CO₂ absorption capacity (molCO₂·L⁻¹ solution) and dissolution rate (mol·s⁻¹) of the solutions were determined by the pressure drop values occurring inside the cell. The experiments were conducted by preparing NaCl solutions at different concentrations (0-3.5 wt%). Additionally, 0.4% by volume calcium oxide (CaO) solution was added to NaCl solutions at different concentrations and its contribution to CO₂ absorption was examined. It was observed that there was a decrease in CO₂ absorption performance with the increase in salinity. However, it was determined that the addition of CaO to the NaCl solution had a positive effect on CO₂ absorption performance and increased the total CO₂ absorption capacity by 66%. The second phase of experiments was carried out in a falling film column. In these experiments, the liquid side individual physical mass transfer coefficients (k_L⁰) were determined by the oxygen (O₂) desorption method for pure water and 3.5 wt% NaCl solution. Also, nonlinear regression analyses were performed, and correlations were developed for mass transfer coefficients.

Article History

Received: 15 Dec 2023

Accepted: 17 Feb 2024

Published: 25 Jun 2024

Research Article

Keywords – Carbon dioxide, absorption, mass transfer coefficient, seawater, calcium oxide

1. Introduction

Climate change resulting from global warming has become an important problem of today. The increase in carbon dioxide (CO₂) concentration in the atmosphere has a large share among the factors causing this problem. A large amount of CO₂ gas is released because of burning fossil fuels, especially for power and energy generation. The issue of CO₂ removal in the fight against climate change is noteworthy and emphasized on international platforms. According to the Intergovernmental Panel on Climate Change (IPCC), CO₂ emissions must reach net zero by 2050 with no or limited temperature rising [1]. In line with the 1.5°C temperature increase and net zero carbon targets set out on international platforms, it is necessary to increase the focus on renewable energy sources and reduce the use of fossil fuels [2, 3]. However, fossil fuels are still used because they are more economic. Also, fossil fuels are directly associated with excessive CO₂ emissions and other toxic gases such as SO₂, H₂S etc. [4, 5]. Therefore, it is important to implement CO₂ removal systems in the fight against climate change.

Ships produce sulfur oxide (SO_x), nitrogen oxide (NO_x), particulate matter and CO₂ emissions due to the fuel they consume in their power and propulsion systems. According to the International Maritime Organization

¹iremkoçyigit@gazi.edu.tr; ²duysal@gazi.edu.tr (Corresponding Author); ³mdogan@gazi.edu.tr; ⁴bzuysal@gazi.edu.tr

(IMO), more than 80% of world trade is carried out by maritime transportation [6]. Maritime transport accounts for 30% of logistics sector emissions and approximately 2-3% of global CO₂ [7]. Reducing CO₂ emissions from ships is important in terms of climate change and environmental pollution.

Carbon capture, utilization, and storage systems (CCUS) are developed technologies [8]. There are three main systems to capture CO₂: pre-combustion, post-combustion, and oxy-fuel combustion [9]. Also, there are many methods to capture CO₂: absorption, adsorption, separation with membrane, cryogenic separation, etc. [10]. Among CO₂ removal systems, CO₂ capture via absorption method in post-combustion systems is one of the most well-known methods [11]. In post-combustion systems, CO₂ is captured by organic solutions such as monoethanolamine (MEA), diethanolamine (DEA), etc. However, amine solutions have several drawbacks related to limited cyclic carbon dioxide loading capacity, degradation by oxygen, high equipment corrosion, and the operating cost is fairly high due to the high energy requirement for regeneration of the solution [12, 13]. The properties of the solutions used in the absorption process greatly affect the cost. These solutions are desired to have low energy costs, high CO₂ selectivity, be environmentally friendly, and have low solution degradation and corrosion [14]. For this reason, efficient alternative solutions are being investigated. Some physical and chemical absorption solutions are widely studied academically and industrial for this purpose [15, 16].

In this study, it is contemplated that the utilization of seawater to capture CO₂ from ship chimneys and processes with high CO₂ emission potential, especially concentrated in the coastal region, will create a potential in terms of environmental impact and cost. The average seawater concentration is 3.5% by mass and most of it is sodium chloride (NaCl). Also, natural seawater is rich in Ca²⁺ and Mg²⁺ ions. The abundance of Ca²⁺ and Mg²⁺ ions in seawater facilitates a direct reaction with CO₂, forming carbonate precipitates for effective CO₂ absorption [17]. This integration combines CO₂ capture with storage and advances the development of CCS (Carbon Capture and Storage) technology. However, the inherent capability of seawater for CO₂ capture is constrained, prompting ongoing research efforts aimed at augmenting the absorption of CO₂ in seawater. To increase the absorption capacity of seawater, researchers have examined the contributions of NH₃, NH₃-NH₄Cl and organic amine solutions [18-20]. However, difficulties such as solution recovery and process complexity have emerged in these studies. Hence, it becomes imperative to explore suitable additives that can augment the CO₂ capture capacity of seawater. The ideal additives should facilitate a straightforward process, yield effective absorption, be cost-effective, generate no by-products, and be environmentally friendly. In this context, it has been seen in the literature that there are studies in which steel slag (SS) with high calcium oxide and magnesium oxide content (~32–58% CaO and 3.9–10.0% MgO) is used as an additive material for CO₂ capture [21, 22]. These additives have potential because of improved CO₂ capture. Since these studies are limited and generally used as additives to fresh water, more research is needed.

This study investigated the CO₂ absorption performance of NaCl solution as seawater and 0.4% v/v CaO + NaCl solution at different concentrations (0-3.5 wt%) in stirred cell. The addition of CaO to the NaCl solution had a positive effect on CO₂ absorption performance and increased the total CO₂ absorption capacity. This study was carried out at atmospheric pressure in Ankara (91 kPa) and ambient temperature (20°C). Also, second phase of experiments was carried out in a falling film column. The liquid side individual physical mass transfer coefficients (k_{L0}) were determined by the oxygen (O₂) desorption method for pure water and 3.5 wt% NaCl solution. Also, nonlinear regression analyses were performed, and correlations were developed for liquid side individual physical mass transfer coefficients.

2. Materials and Methods

In this study, experiments were carried out in two stages and the CO₂ absorption performance of sodium chloride (NaCl) solution as seawater was investigated. A stirred cell system was used to assess the CO₂ absorption performance of NaCl solutions. In stirred cell experiments, NaCl solutions were prepared in a range of low and high concentrations based on seawater salinity levels (0-3.5 wt%). Stirred cell experiments were carried out at 91 kPa pressure (atmospheric pressure in Ankara) and 20°C temperature. In falling film column experiments, liquid side individual physical mass transfer coefficients (k_L^0) were determined by the oxygen (O₂) desorption method for pure water and 3.5 wt% NaCl solutions. Falling film column experiments were carried out 91 kPa pressure (atmospheric pressure in Ankara) and 18°C temperature.

2.1. Stirred Cell Experiments

2.1.1. Experimental Set-Up

Experiments were carried out in a stirred cell system. The stirred cell is a known equipment for gas-liquid interaction systems [23, 24]. The stirred cell system operates on the principle of trapping the gas in the gas chamber and allowing it to be absorbed by the solution in the liquid reservoir. By observing the amount of gas absorbed by the solution and the pressure drop in the gas chamber, it is possible to determine how much gas has been absorbed. The schematic experimental set-up is shown in Figure 1.

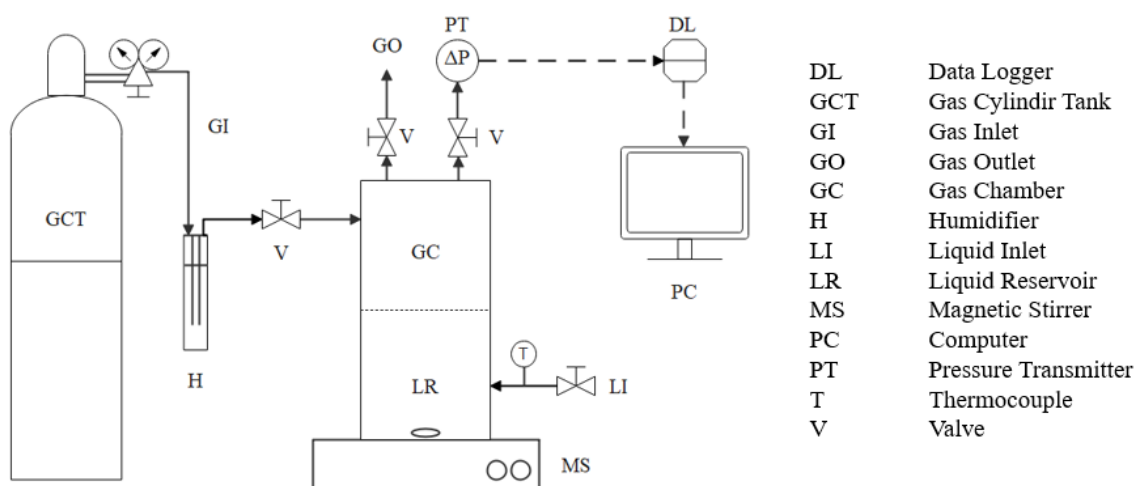


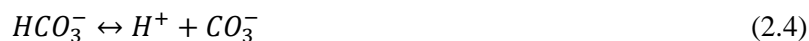
Figure 1. The stirred cell system

The stirred cell system consists of two parts, a gas chamber (0.5 L) and a liquid reservoir (0.4 L). The stirred cell is made of pyrex glass. The gas chamber has valves to which the gas inlet and outlet are connected. A CO₂ gas cylinder (>99.99%) is attached to the gas chamber. Before the gas was fed to the cell, the gas was passed through a humidifier to saturate the gas to water vapor. The absorption liquid is placed in the liquid reservoir. The two sections of the system are sealed together using a metal clamp. Throughout the experiments, the absorption liquid was stirred at a very low speed using a VELP SCIENTIFICA ARE model magnetic stirrer. The pressure drop in the cell was monitored using an HK Instruments DPT-R8 model differential pressure transmitter and recorded on the computer via the ORDEL UDL100 model data logger. Weight measurements were conducted using an analytical balance with an accuracy of ±0.1 mg.

2.1.2. Experimental Procedure

In the experiments, pure CO₂ gas flow was initially introduced into the stirred cell through the gas inlet to purge the air from the system. Subsequently, all valves were simultaneously closed, trapping the CO₂ gas in the gas chamber. Then, trapped CO₂ gas in the system was absorbed into the absorption solution. As CO₂ was absorbed, the pressure in the gas chamber gradually decreased until it stabilized at a constant value. Meanwhile, the absorption solution was stirred using a magnetic stirrer ensuring no vibration or vortex formation at the interface. This stirring served to prevent any potential mass transfer resistances that might occur at the liquid surface or in close proximity to it, providing homogeneity within the liquid. Additionally, the solution's temperature was continuously monitored by a thermocouple with an accuracy of ±0.2 K. During the experiments, the pressure in the gas chamber was recorded every second on the computer using a data logger and a differential pressure transmitter. While the pressure drop values initially increased over time in the stirred cell, they eventually stabilized. Subsequently, the total CO₂ absorption capacity and dissolution rate were calculated using the recorded data.

CO₂ dissolution in seawater occurs in a few steps. Dissolved CO₂ (in aqueous form as shown in (2.1)) in seawater converts to carbonic acid (H₂CO₃), carbonate (CO₃²⁻) and bicarbonate (HCO₃⁻) ions as shown in (2.2)-(2.4), respectively. Then, carbonate (CO₃²⁻), Ca²⁺ and Na²⁺ ions in seawater form precipitation in solution as shown in (2.5) and (2.6).



2.1.3. Total CO₂ Absorption Capacity

To determine the pressure in the gas chamber, the ideal gas equation (shown in (2.7)) was used by correcting for real gases by using the compressibility factor [25].

$$PV_g = ZnRT \quad (2.7)$$

In this equation, P is the gas pressure [Pa] in the stirred cell gas chamber; V_g is the gas volume [m³], Z is the compressibility factor [0.995], n is the mole of carbon dioxide gas [mol], R is the gas constant [8.314 Pa·m³·mol⁻¹·K⁻¹], T is the temperature [K]. The compressibility factor (Z) in the ideal gas equation was calculated by taking into account the composition of pure CO₂ gas passed through the humidifier. The compressibility factor (Z) according to the composition value of water-saturated CO₂ gas was calculated with the help of the Peng-Robinson model [26].

The pressure in the gas chamber of the stirred cell is equal to the difference between atmospheric pressure and pressure drop value which is shown in (2.8).

$$P = P_{atm} - \Delta P \quad (2.8)$$

The pressure drop values in the gas chamber were recorded on the computer via the differential pressure transmitter. Then these data were plotted against the time that is shown in Figure 2 as an example. The ordinate of the graph represents the pressure drop difference (ΔP) measured from the transmitter in Pa units, and the abscissa represents the time in seconds.

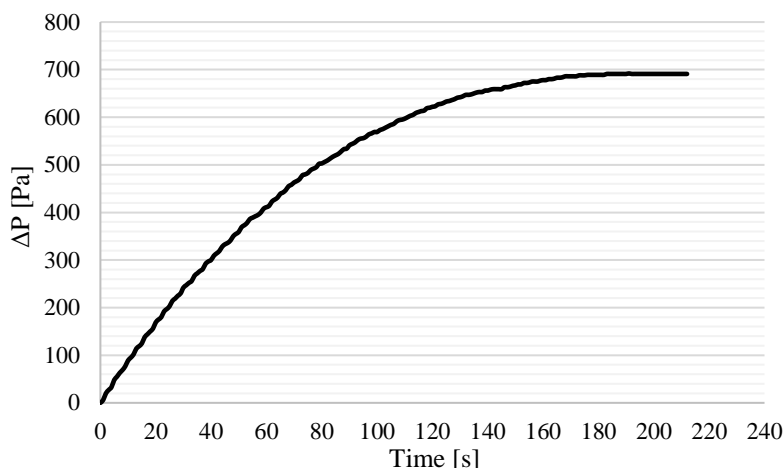


Figure 2. Increase in pressure drop (ΔP) in the gas chamber of the stirred cell with time

With the help of the pressure drop values fixed at the end of the experiment, the mole of CO_2 gas remaining in the gas chamber was calculated with (2.7). After that, by taking the difference between gas moles in the initial and final state, the amount of CO_2 absorbed into the unit volume of absorption liquid was determined [27].

2.1.4. Dissolution Rate

The dissolution rate experimental procedure is similar to the total CO_2 absorption capacity experiments but theoretically different. (2.9) is obtained by taking and arranging the differential of (2.7) [28].

$$dn = \frac{V_g}{ZRT} dP \quad (2.9)$$

Since the experiments are conducted as a function of time, the change of the expression obtained by (2.9) with time is shown in (2.10) [28].

$$w = \frac{dn}{dt} = \frac{V_g}{ZRT} \frac{dP}{dt} \quad (2.10)$$

Here, w is the dissolution rate [$\text{mol}\cdot\text{s}^{-1}$] of CO_2 in the absorption solutions. The part on the right side of the equation expresses the change in moles of CO_2 due to the absorption of CO_2 in the gas chamber into the absorption solutions over time.

The internal pressure in the gas chamber was determined with (2.8) and the internal pressure changing plot is shown in Figure 3. To determine the pressure change (dP/dt) over time, the slope of the first part of the graph, in which it proceeds linearly, was taken. Then, this value is used in Equations (2.10) and (2.11).

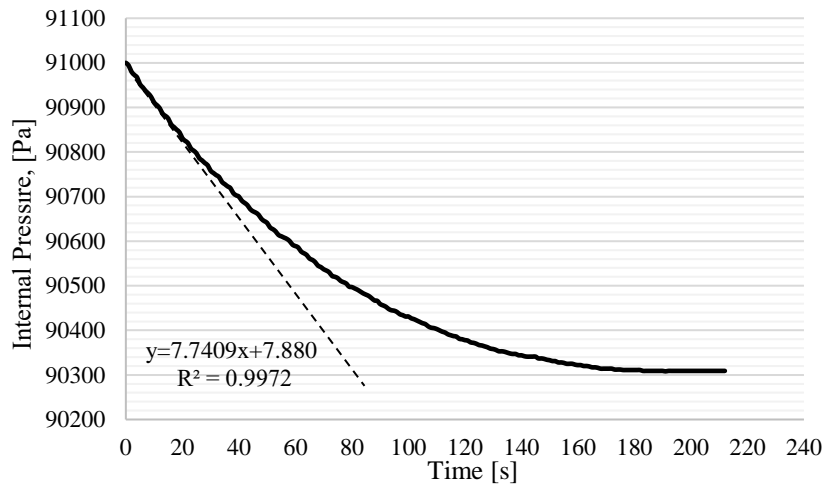


Figure 3. The change in the internal pressure (P) in the gas chamber of the stirred cell with time

The absorption occurred in the liquid reservoir volume (V_L), and the dissolution rate of CO_2 in the solution can be shown by (2.11) [28].

$$r = \frac{w}{V_L} = -\frac{1}{V_L} \frac{V_g}{zRT} \frac{dP}{dt} \quad (2.11)$$

Here, r is the rate of the absorption process relative to the total solution volume in the unit $[\text{mol} \cdot \text{m}^{-3} \cdot \text{s}^{-1}]$, the slope read from the graph in the unit of dP/dt $[\text{Pa} \cdot \text{s}^{-1}]$ on the right side of the equation, V_L , solution volume $[\text{m}^3]$, V_g , gas volume $[\text{m}^3]$, T is the temperature in $[\text{K}]$, R is the gas constant $[8.314 \text{ Pa} \cdot \text{m}^3 \cdot \text{mol}^{-1} \cdot \text{K}^{-1}]$.

2.2. Falling Film Column Experiments

2.2.1. Experimental Set-Up

Liquid side individual physical mass transfer coefficients (k_L^0) were determined by the O_2 desorption method in falling film column. O_2 desorption method is known in literature for determining k_L^0 [29, 30]. The falling film column used in the experiments is similar in concept with wetted wall columns. Wetted wall column are frequently used equipment in mass transfer studies because they are easy to design and provide a high mass transfer rate [31, 32]. The schematic falling film columns experimental set-up is shown in Figure 4.

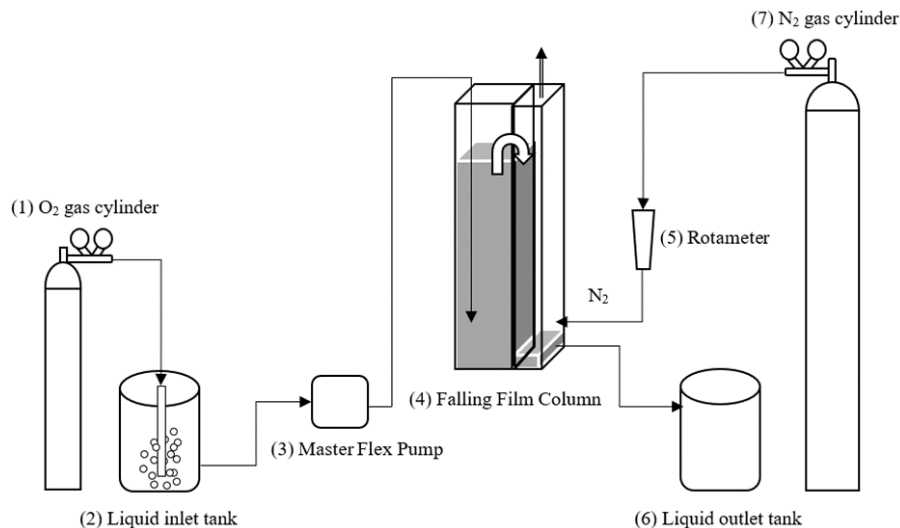


Figure 4. The falling film column system

The falling film column system consists of two different parts separated in the middle by a plate. The dimensions of the liquid chamber of the system are 55x200x60 mm and the dimensions of the gas chamber are 20x200x60 mm. The falling film column is made of plexiglass. To ensure smooth laminar flow over the plate in the middle, gas velocities are determined hydrodynamically as 0.0069, 0.0139, 0.0208, 0.0278, 0.0347 m·s⁻¹ and liquid velocities 0.00606, 0.00808, 0.0101, 0.0121 m·s⁻¹. For the determination of the concentration of O₂ in the liquid inlet and outlet, a portative YSI Model 50B Dissolved Oxygen Meter was used.

2.2.2. Experimental Procedure

In the experiments, distilled water and sea water saturated with O₂ gas cylinder are fed to the system as liquid. During the laminar film flow over the middle plate, the dissolved oxygen in the liquid was desorbed into the nitrogen gas fed from the gas inlet of the system. During the experiments, three water samples for each gas velocity (into the 5 mL beakers) were obtained from the inlet and the outlet of the falling film column, and the concentration of O₂ in the liquid was measured instantaneously with a portative O₂ analyser. Experiments were carried out in 5 different gas and 4 different liquid velocities at 18°C temperature. Then, using the concentration of O₂ in the liquid, liquid side individual physical mass transfer coefficients were calculated.

2.2.3. Liquid Side Individual Physical Mass Transfer Coefficient

To determine the amount of O₂ passing from liquid to gas, the flux expression according to the two-resistance theory can be shown as (2.12).

$$\overline{N}_A = k_L^0 C_T (x_A - x_{A,i})_{LM} \quad (2.12)$$

where \overline{N}_A is the average flux [kmol·m⁻²·s⁻¹], k_L^0 is liquid side individual physical mass transfer coefficient [m·s⁻¹], C_T is the total concentration [kmol·m⁻³], x_A [-] and $x_{A,i}$ are the mole fractions of liquid phase O₂ and the interfacial composition at the liquid side in equilibrium with the gas side O₂ composition, respectively.

If (2.12) is arranged, the liquid side individual physical mass transfer coefficients were calculated using (2.13).

$$k_L^0 = \frac{\overline{N}_A}{C_T(x_1 - x_2)} \ln \frac{(x_1 - x_i)}{(x_2 - x_i)} \quad (2.13)$$

where x_1 and x_2 are the mole fractions of liquid phase O₂ at the inlet and outlet of the column, respectively. x_i value which is constant for the experimental temperature can be found in the literature, yet it was corrected for the ambient pressure [28]. According to both penetration and surface renewal theories in the literature, the mass transfer coefficient is directly proportional to the square root of the diffusion coefficient [33]. Therefore, the liquid side individual physical mass transfer coefficient of the CO₂ can be estimated using the correction factor as shown in (2.14) [33].

$$(k_L^0)_{CO_2} = (k_L^0)_{O_2} \sqrt{\frac{D_{CO_2-H_2O}}{D_{O_2-H_2O}}} \quad (2.14)$$

The diffusion coefficient of CO₂ in distilled water ($D_{CO_2-H_2O}$) can be calculated as in (2.15) through the correlation developed by Versteeg and Van Swaaij, where the temperature is in [K] [34].

$$D_{\text{CO}_2-\text{H}_2\text{O}} = 2.35 \times 10^{-6} e^{-\frac{2119}{T}} \quad (2.15)$$

The diffusion coefficient of O₂ in water (D_{O₂-H₂O}) was calculated by the Wilke-Chang equation as shown in (2.16) [33].

$$D_{\text{O}_2-\text{H}_2\text{O}} = 1.17 \times 10^{-13} \frac{\sqrt{\psi_B M_B T}}{\mu V_A^{0.6}} \quad (2.16)$$

where D_{AB} [m²·s⁻¹] is diffusion coefficient, M_B [kg·kmol⁻¹] is the molecular weight of the solvent, T [K] is temperature, V_A [m³·kmol⁻¹] is the molar volume of solute at normal boiling temperature, μ [cp] is the viscosity of the solution and ψ_B [-] is association parameter for solvent B. Literature data from [35] were used for the diffusion coefficient of CO₂ in seawater at 18°C.

3. Results and Discussion

3.1. Total CO₂ Absorption Capacity and Dissolution Rate

As the result of stirred cell experiments, the dissolution rate (w), the rate of the absorption process relative to the total liquid volume (r), and the total CO₂ absorption capacity were calculated. All experiments were repeated 3 times and since the values are close to each other, the average values were determined for each solution. Firstly, 0-3.5 wt% NaCl experiments were carried out in stirred cell reactor. The results of the 0-3.5 wt% NaCl experiment are shown in Table 1.

Table 1. Experimental results of total CO₂ absorption capacity and dissolution rate for 0-3.5 wt% NaCl solutions

Solution	w* (mol/s)	r** (mol/m ³ ·s)	Total CO ₂ absorption capacity (mol/L)
0 wt% NaCl (distilled-water)	2.90 x10 ⁻⁶	0.0580	0.0048
0.5 wt% NaCl	2.70 x10 ⁻⁶	0.0539	0.0046
1 wt% NaCl	2.65 x10 ⁻⁶	0.0530	0.0045
1.5 wt% NaCl	2.61 x10 ⁻⁶	0.0526	0.0044
2 wt% NaCl	2.58 x10 ⁻⁶	0.0517	0.0040
2.5 wt % NaCl	2.48 x10 ⁻⁶	0.0496	0.0040
3 wt % NaCl	2.43 x10 ⁻⁶	0.0487	0.0039
3.5 wt % NaCl	2.42 x10 ⁻⁶	0.0485	0.0038

*Dissolution rate

**The rate of the absorption process relative to the total liquid volume

The experimental results of the 0-3.5 wt% NaCl solutions are also shown in Figure 5 graphically.

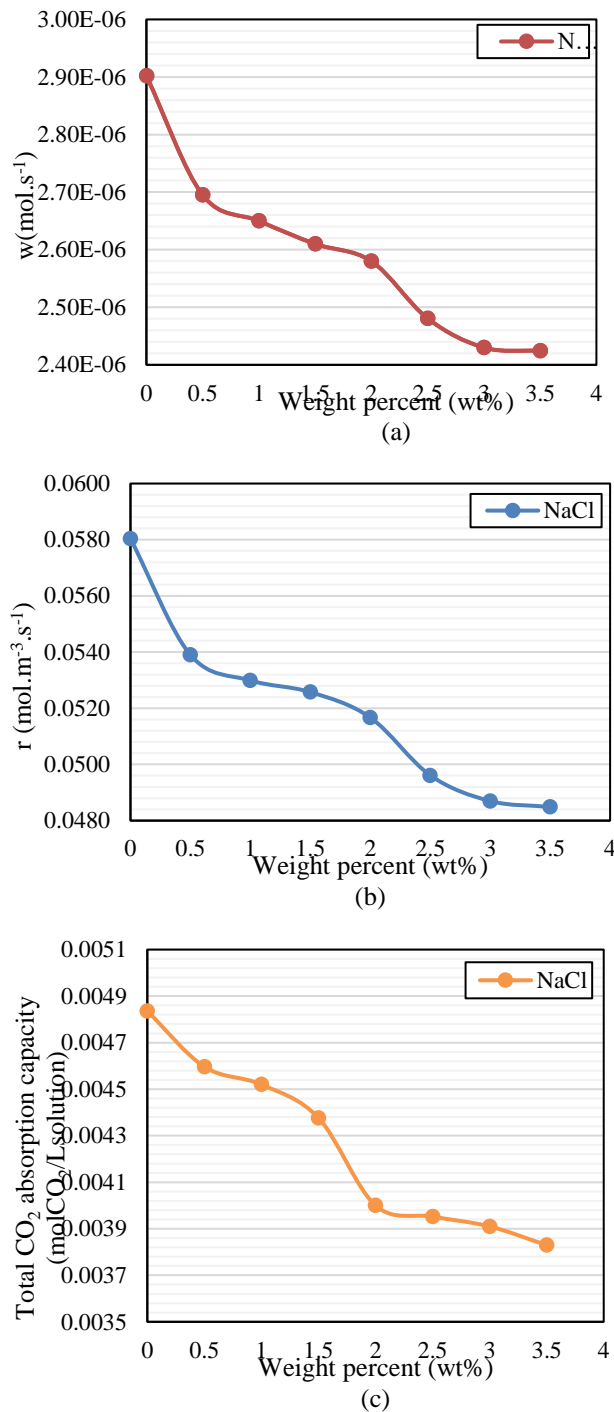


Figure 5. (a) The dissolution rate of CO₂ of 0-3.5 wt% NaCl solutions; (b) The rate of the absorption process relative to the total solution volume of 0-3.5 wt% NaCl solutions; (c) Total CO₂ absorption capacity of 0-3.5 wt% NaCl solutions

When Figure 5 is examined, the most striking result is the observation of a decreasing trend in absorption capacity and dissolution rate with increasing salinity. This result was compared with the literature and Li et al. [17] reported that Henry's constant increased and CO₂ solubility decreased with increasing salinity. Dissolved carbonate and bicarbonate ions in water will form more sodium carbonate in the presence of high salt concentration. For this reason, it can be said that there are more free carbonate and bicarbonate ions in water with lower salt concentrations. Therefore, it is an expected result that CO₂ absorption capacity decreases with increasing salinity.

Subsequently, the experiments were repeated by adding 0.4 v/v% CaO solution to 0-3.5 wt% NaCl solution. The results of the 0-3.5 wt% NaCl + 0.4 v/v% CaO solutions experiments are shown in Table 2.

Table 2. Experimental results of total CO₂ absorption capacity and dissolution rate for 0-3.5 wt% NaCl + 0.4 v/v% CaO solutions

Solution	w* (mol/s)	r** (mol/m ³ .s)	Total CO ₂ absorption capacity (mol/L)
0.5 wt% NaCl + 0.4 v/v% CaO	6.97 x10 ⁻⁶	0.1395	0.01366
1 wt% NaCl + 0.4 v/v% CaO	6.67 x10 ⁻⁶	0.1322	0.01345
1.5 wt% NaCl + 0.4 v/v% CaO	6.54 x10 ⁻⁶	0.1308	0.01293
2 wt% NaCl + 0.4 v/v% CaO	6.41 x10 ⁻⁶	0.1281	0.01232
2.5 wt % NaCl + 0.4 v/v% CaO	6.15 x10 ⁻⁶	0.1229	0.01161
3 wt % NaCl + 0.4 v/v% CaO	5.20 x10 ⁻⁶	0.0998	0.00890
3.5 wt % NaCl + 0.4 v/v% CaO	4.82 x10 ⁻⁶	0.0964	0.00830

*Dissolution rate
 **The rate of the absorption process relative to the total liquid volume

The comparison results of the 0-3.5 wt% NaCl and 0-3.5 wt% NaCl + 0.4 v/v% CaO solutions are also shown in graphically Figure 6.

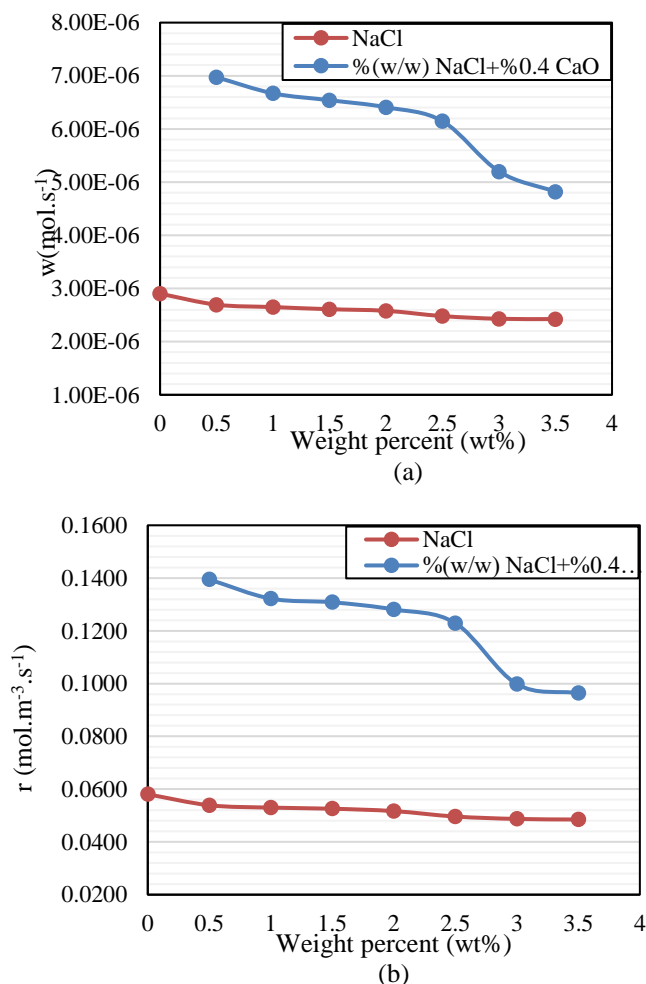


Figure 6. (a) The dissolution rate comparison of CO₂ of 0-3.5 wt% NaCl and 0-3.5 wt% NaCl + 0.4 v/v% CaO solutions; (b) The rate of the absorption process relative to the total solution volume comparison of 0-3.5 wt% NaCl and 0-3.5 wt% NaCl + 0.4 v/v% CaO solutions; (c) Total CO₂ absorption capacity comparison of 0-3.5 wt% NaCl and 0-3.5 wt% NaCl + 0.4 v/v% CaO solutions

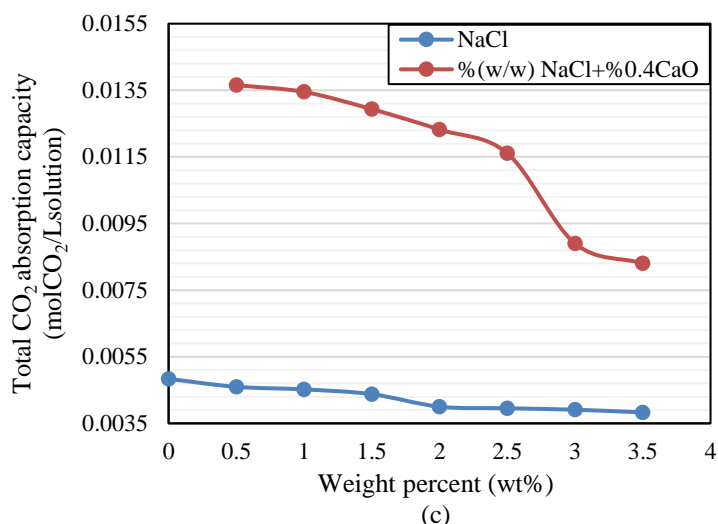


Figure 6. (Continued) (a) The dissolution rate comparison of CO₂ of 0-3.5 wt% NaCl and 0-3.5 wt% NaCl + 0.4 v/v% CaO solutions; (b) The rate of the absorption process relative to the total solution volume comparison of 0-3.5 wt% NaCl and 0-3.5 wt% NaCl + 0.4 v/v% CaO solutions; (c) Total CO₂ absorption capacity comparison of 0-3.5 wt% NaCl and 0-3.5 wt% NaCl + 0.4 v/v% CaO solutions

When Figure 6 is examined, it is clearly seen that CaO contribution to salty seawater has a positive effect. Seawater does not have the ability to form sufficient carbonate deposits itself. By dissolving in seawater, CaO increases the alkalinity of the water and increases the formation of carbonate and bicarbonate ions by promoting carbonic acid ionization in seawater. Increasing carbonate and bicarbonate ions also have a positive effect on CO₂ absorption potential. According to the results obtained, CaO addition increased the total CO₂ absorption capacity by 66%.

3.2. Liquid Side Individual Physical Mass Transfer Coefficient

As a result of falling film column experiments, liquid side individual physical mass transfer coefficients were calculated. The results of diffusion coefficient of CO₂ in distilled water and 3.5 wt% NaCl solution are shown in Table 3.

Table 3. Diffusion coefficients of distilled water, seawater and oxygen

$D_{CO_2-H_2O}(\text{distilled water})$ (m ² -s ⁻¹)	$D_{CO_2-H_2O}(\text{seawater})$ (m ² -s ⁻¹)	$D_{O_2-H_2O}(\text{distilled water})$ (m ² -s ⁻¹)	$D_{O_2-H_2O}(\text{seawater})$ (m ² -s ⁻¹)
1.617 x 10 ⁻⁹	1.384 x 10 ⁻⁹	2.780 x 10 ⁻⁹	2.931 x 10 ⁻⁹

The experimental results of the distilled water and 3.5 wt% NaCl solution with diffusion correction factor applied are shown in Figures 7 and 8, respectively.

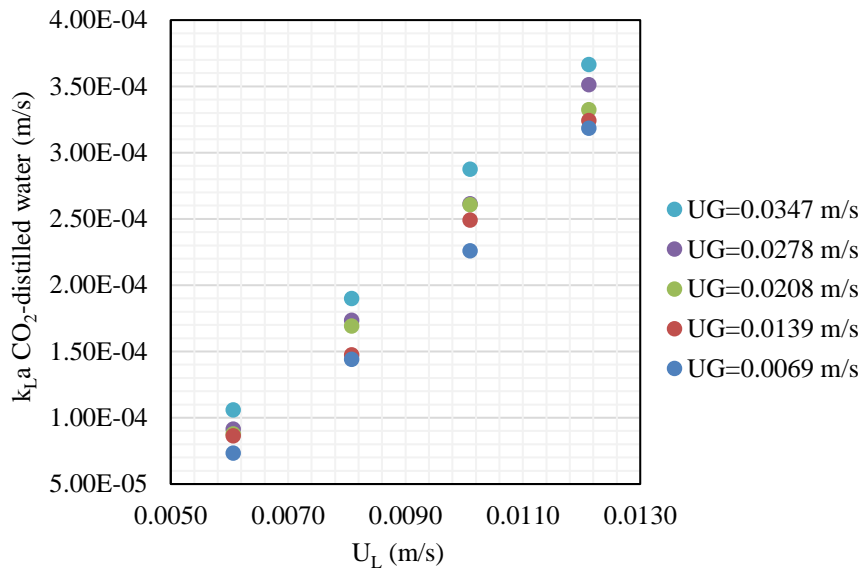


Figure 7. The liquid side individual physical mass transfer coefficients at different gas and liquid velocities by using oxygen desorption method-distilled water

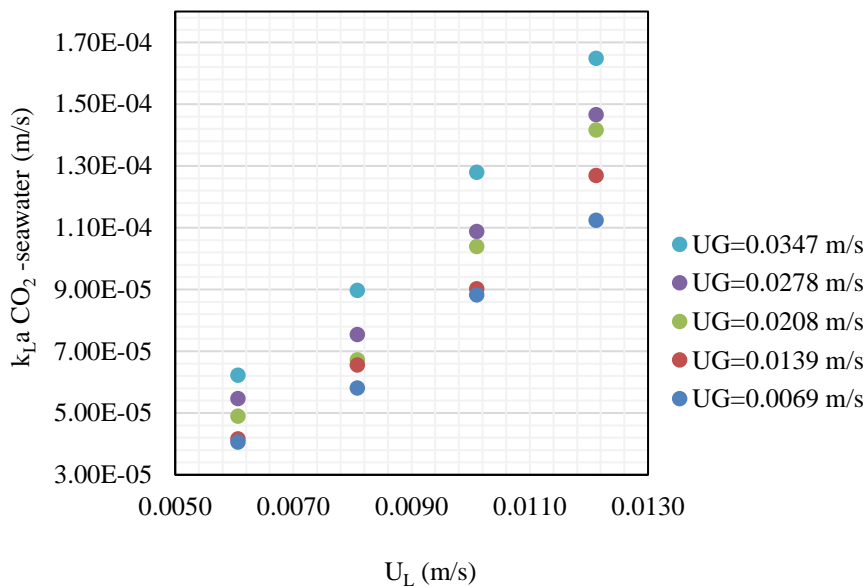


Figure 8. The liquid side individual physical mass transfer coefficients at different gas and liquid velocities by using oxygen desorption method-3.5 wt% NaCl solutions (as a seawater)

With the data obtained, the following correlation for the liquid side individual physical mass transfer coefficient of the CO₂ in water was developed with the nonlinear regression analysis and the regression coefficient was R²=0.974.

$$k_{L(CO_2-distilled\ water)}^0 = 1.230 U_L^{1.829} U_G^{0.031} \quad (3.1)$$

With the data obtained, the following correlation for the liquid side individual physical mass transfer coefficient of the CO₂ in 3.5 wt% NaCl solution (as a seawater) was developed with the nonlinear regression analysis and the regression coefficient was R²=0.904.

$$k_{L(CO_2-seawater)}^0 = 0.153 U_L^{1.543} U_G^{0.057} \quad (3.2)$$

As can be seen from the results, liquid side individual physical mass transfer coefficient correlations vary depending on both liquid and gas velocities. While the gas effect dominates at low liquid velocities, the liquid effect becomes dominant at high liquid velocities and the gas effect remains in the background. In this study, the liquid velocity operating range is higher than the gas velocity. Therefore, it is an expected result that the correlations are dependent on the liquid velocity. There are many k_L^0 correlations for distilled water in the literature and k_L^0 varies between $0.4-10 \times 10^{-4}$ [$m \cdot s^{-1}$] [28, 36, 37]. The results obtained from this study are in agreement with the literature. There are limited number of studies in the literature on the physical individual mass transfer coefficient of seawater. In their study, Cho & Choi [38] obtained k_L^0 in the range of $7.7-9.2 \times 10^{-5}$ [$m \cdot s^{-1}$] on average under 3-4 bar conditions. These results are similar to the results of this study in terms of order of magnitude.

4. Conclusion

In this study, experiments were carried out in two stages which are stirred cell and falling film column. In the stirred cell, the experiments were conducted at a concentration range of 0-3.5 wt% NaCl solutions and by adding CaO to NaCl solutions at the same concentration. When the experimental results were evaluated, it was observed that there was a decrease in CO₂ absorption performance as the salinity increased. When compared with the literature, it was seen that the study was in the same direction as the literature in terms of the effect of salinity. In the study, it was aimed to increase the CO₂ absorption capacity of the solution by adding CaO to the solution to increase the Ca⁺² ion in the NaCl solution. As a result of the experiments, it was seen that adding CaO to NaCl solution had a positive effect on the results of total CO₂ absorption capacity ($molCO_2 \cdot L^{-1}$ solution) and dissolution rate ($mol \cdot s^{-1}$). When evaluated in terms of total CO₂ absorption capacity, it was determined that CaO-doped NaCl solutions absorbed CO₂ 66% better than the pure NaCl solution. In the falling film column, the liquid side individual physical mass transfer coefficients (k_L^0) were determined by the oxygen (O₂) desorption method for pure water and 3.5 wt% NaCl solution. The results obtained were found to be compatible with the literature. Also, nonlinear regression analyses were performed, and correlations were developed for liquid side individual physical mass transfer coefficients.

Author Contributions

The first author collected data, performed the analysis, and wrote the paper. The second author conceived analysis, methodology, formal analysis, and review and edit of the paper. The third author also conceived the analysis and formal analysis. The fourth author designed the analysis and methodology. They all read and approved the final version of the paper.

Conflicts of Interest

All the authors declare no conflict of interest.

Acknowledgement

The authors would like to thank Hazel Sarihan for her help in getting some experimental data for this study.

References

- [1] IPCC, *Climate Change 2022: Impacts, Adaptation and Vulnerability*, in: H.-O. Pörtner, D. C. Roberts, M. Tignor, E. S. Poloczanska, K. Mintenbeck, A. Alegría, M. Craig, S. Langsdorf, S. Löschke, V. Möller, A. Okem, B. Rama (Eds.), Contribution of Working Group II to the Sixth Assessment Report of the Intergovernmental Panel on Climate Change, Switzerland, 2022, 35 pages.
- [2] IPCC, *Global Warming of 1.5°C*, in: Masson-Delmotte, V., P. Zhai, H.-O. Pörtner, D. Roberts, J. Skea, P.R. Shukla, A. Pirani, W. Moufouma-Okia, C. Péan, R. Pidcock, S. Connors, J.B.R. Matthews, Y. Chen, X. Zhou, M.I. Gomis, E. Lonnoy, T. Maycock, M. Tignor, and T. Waterfield (Eds.) Intergovernmental Panel on Climate Change, Switzerland, 2018, pp. 541–562.
- [3] H. Öztan, İ. Koçyiğit Çapoğlu, D. Uysal, Ö. M. Doğan, *A parametric study to optimize the temperature of hazelnut and walnut shell gasification for hydrogen and methane production*, Bioresource Technology Reports 23 (2023) 101581.
- [4] Ö. Yörük, D. Uysal Zıraman, B. Z. Uysal, *Absorption of sulfur dioxide by iron(ii) hydroxide solution in a multiplate bubble column under magnetic field*, Chemical Engineering & Technology 44 (1) (2021) 1336–1342.
- [5] Y. Yagizatli, B. Ulas, A. Sahin, İ. Ar, *Investigation of sulfonation reaction kinetics and effect of sulfonation degree on membrane characteristics for PEMFC performance*, Ionics 28 (5) (2022) 2323–2336.
- [6] R. Baumler, M. C. Arce, A. Pazaver, *Quantification of influence and interest at IMO in Maritime Safety and Human Element matters*, Marine Policy 133 (2021) 104746 12 pages.
- [7] H. Al Baroudi, A. Awoyomi, K. Patchigolla, K. Jonnalagadda, E. J. Anthony, *A review of large-scale CO₂ shipping and marine emissions management for carbon capture, utilisation and storage*, Applied Energy 287 (2021) 116510 42 pages.
- [8] Z. Zhang, D. Huisinigh, *Carbon dioxide storage schemes: Technology, assessment and deployment*, Journal of Cleaner Production 142 (2) (2017) 1055–1064.
- [9] A. A. Olajire, *CO₂ capture and separation technologies for end-of-pipe applications—A review*, Energy 35 (6) (2010) 2610–2628.
- [10] J. Buckingham, T. R. Reina, M. S. Duyar, *Recent advances in carbon dioxide capture for process intensification*, Carbon Capture Science & Technology 2 (95) (2022) 100031 19 pages.
- [11] F. O. Ochedi, J. Yu, H. Yu, Y. Liu, A. Hussain, *Carbon dioxide capture using liquid absorption methods: a review*, Environmental Chemistry Letters 19 (2021) 77–109.
- [12] S. Ahn, H. J. Song, J. W. Park, J. H. Lee, I. Y. Lee, K. R. Jang, *Characterization of metal corrosion by aqueous amino acid salts for the capture of CO₂*, Korean Journal of Chemical Engineering, 27 (5) (2010) 1576–1580.
- [13] I. M. Bernhardsen, H. K. Knuutila, *A review of potential amine solvents for CO₂ absorption process: absorption capacity, cyclic capacity and pKa*, International Journal of Greenhouse Gas Control 61 (2017) 27–48.
- [14] M. Wang, A. Lawal, P. Stephenson, J. Sidders, C. Ramshaw, *Post-combustion CO₂ capture with chemical absorption: A state-of-art review*, Chemical Engineering Research and Design 89 (9) (2011) 1609–1624.
- [15] D. Uysal, Ö. M. Dogan, B. Z. Uysal, *Kinetics of absorption of carbon dioxide into sodium metaborate solution*, International Journal of Chemical Kinetics 49 (6) (2017) 377–386.
- [16] G. Genç Çelikçi, D. Uysal, B. Z. Uysal, *Absorption of carbon dioxide into n-butanol and ethyl acetate in a column with structured packing*, Chemical Engineering & Technology 45 (8) (2022) 1489–1496.

- [17] H. Li, Z. Tang, N. Li, L. Cui, X-Z. Mao, *Mechanism and process study on steel slag enhancement for CO₂ capture by seawater*, Applied Energy 276 (2020) 115515 14 pages.
- [18] M. H. El-Naas, A. H. Al-Marzouqi, O. Chaalal, *A combined approach for the management of desalination reject brine and capture of CO₂*, Desalination 251 (1-3) (2010) 70–74.
- [19] W. Wang, M. Hu, Y. Zheng, P. Wang, C. Ma, *CO₂ fixation in Ca²⁺-/Mg²⁺-rich aqueous solutions through enhanced carbonate precipitation*, Industrial & Engineering Chemistry Research 50 (13) (2011) 8333–8339.
- [20] W. Wang, X. Liu, P. Wang, Y. Zheng, M. Wang, *Enhancement of CO₂ Mineralization in Ca²⁺-/Mg²⁺-rich aqueous solutions using insoluble amine*, Industrial & Engineering Chemistry Research 52 (23) (2013) 8028–8033.
- [21] A. Said, H. -P. Mattila, M. Järvinen, R. Zevenhoven, *Production of precipitated calcium carbonate (PCC) from steelmaking slag for fixation of CO₂*, Applied Energy 112 (2013) 765–771.
- [22] A. Said, T. Laukkanen, M. Järvinen, *Pilot-scale experimental work on carbon dioxide sequestration using steelmaking slag*, Applied Energy 177 (1) (2016) 602–611.
- [23] L. Kucka, J. Richter, E. Y. Kenig, A. Górak, *Determination of gas–liquid reaction kinetics with a stirred cell reactor*, Separation & Purification Technology 31 (2) (2003) 163–175.
- [24] J. Ying, D. A Eimer. *Determination and measurements of mass transfer kinetics of CO₂ in concentrated aqueous monoethanolamine solutions by a stirred cell*, Industrial & Engineering Chemistry Research 52 (7) (2013) 2548–2559.
- [25] J. M. Smith, H. C. Van Ness, M. M. Abbott, M. T. Swihart, *Introduction to chemical engineering thermodynamics*, Mc Graw-Hill, New York, 2022.
- [26] S. I. Sandler, *Chemical, biochemical and engineering thermodynamics*, 4th Edition, John Wiley & Sons Inc., New York, 2006.
- [27] G. Genç Çelikçi, *Carbon dioxide capture in structured packing column with n-butanol and ethyl acetate*, Doctoral Dissertation Gazi University (2020) Ankara.
- [28] D. Uysal, *Absorption of carbon dioxide into calcium acetate solution*, Doctoral Dissertation Gazi University (2016) Ankara.
- [29] A. H. G. Cents, F. T. de Bruijn, D. W. F. Brilman, G. F. Versteeg, *Validation of the Danckwerts-plot technique by simultaneous chemical absorption of CO₂ and physical desorption of O₂*, Chemical Engineering Science 60 (21) (2005) 5809–5818.
- [30] A. Hoffmann, J. Maćkowiak, A. Gorak, M. Haas, J. M. Löning, T. Runowski, K. Hallenberger, *Standardization of mass transfer measurements: a basis for the description of absorption processes*, Chemical Engineering Research & Design 85 (1) (2007) 40–49.
- [31] C. D. Park, T. Nosoko, *Three-dimensional wave dynamics on a falling film and associated mass transfer*, AIChE Journal 49 (11) (2003) 2715–2727.
- [32] C. Wang, Z. Xu, C. Lai, X. Sun, *Beyond the standard two-film theory: Computational fluid dynamics simulations for carbon dioxide capture in a wetted wall column*, Chemical Engineering Science 184 (2018) 103–110.
- [33] B. Z. Uysal, *Mass transfer-fundamentals and applications (in Turkish)*, 3th Edition, Gazi Kitabevi, Ankara, 2019.
- [34] G. F., Versteeg, W. P. Van Swaaij, *Solubility and diffusivity of acid gases (carbon dioxide, nitrous oxide) in aqueous alkanolamine solutions*, Journal of Chemical Engineering Data 33 (1988) 29–34.

- [35] A. Poisson, A. Papaud, *Diffusion coefficients of major ions in seawater*, Marine Chemistry 13 (4) (1983) 265–280.
- [36] A. P. Lamourelle, O. C. Sandall, *Gas absorption into a turbulent liquid*, Chemical Engineering Science 27 (5) (1972) 1035–1043.
- [37] S-M. Yih, K. -Y. Chen, *Gas absorption into wavy and turbulent falling liquid films in a wetted-wall column*, Chemical Engineering Communications 17 (1-6) (1982) 123–136.
- [38] H. -J. Cho, J. Choi, *Calculation of the mass transfer coefficient for the dissolution of multiple carbon dioxide bubbles in sea water under varying conditions*, Journal of Marine Science and Engineering 7 (12) (2019) 457 11 pages.